



Modulation of the antitumor immune response by complement

Maciej M Markiewski¹, Robert A DeAngelis¹, Fabian Benencia^{2,4}, Salome K Ricklin-Lichtsteiner¹, Anna Koutoulaki¹, Craig Gerard³, George Coukos² & John D Lambris¹

The involvement of complement-activation products in promoting tumor growth has not yet been recognized. Here we show that the generation of complement C5a in a tumor microenvironment enhanced tumor growth by suppressing the antitumor CD8⁺ T cell-mediated response. This suppression was associated with the recruitment of myeloid-derived suppressor cells into tumors and augmentation of their T cell-directed suppressive abilities. Amplification of the suppressive capacity of myeloid-derived suppressor cells by C5a occurred through regulation of the production of reactive oxygen and nitrogen species. Pharmacological blockade of the C5a receptor considerably impaired tumor growth to a degree similar to the effect produced by the anticancer drug paclitaxel. Thus, our study demonstrates a therapeutic function for complement inhibition in the treatment of cancer.

The diverse functions of the immune system in cancer initiation and development are illustrated by two ideas: the ‘cancer immunoeediting’ theory, which postulates that the immune system protects the host against cancer development^{1,2}, and the traditional idea that long-lasting inflammatory reactions facilitate malignant transformation and cancer progression^{3–6}. Although an immune reaction develops against malignant tumor cells, tumors can suppress this immune response and escape from immune effector mechanisms^{2,7,8}. Antigen-specific CD8⁺ T cell tolerance induced by myeloid-derived suppressor cells (MDSCs) recruited by tumors is an example of one such suppression mechanism^{9,10}. Although the mechanisms responsible for the suppressive phenotype of MDSCs vary, several studies have postulated that MDSCs produce large quantities of reactive oxygen species (ROS) or reactive nitrogen species (RNS), which directly inhibit the antigen-specific CD8⁺ T cell-dependent immune response¹¹. In addition, the metabolism of L-arginine regulated by arginase-1 contributes to the generation of these reactive species and seems to be central to the suppression of T cells by MDSCs¹². The immunosuppressive ability of MDSCs is thought to be one of the main obstacles that limits the use of anticancer vaccines⁵.

Another potential participant in the response to cancer is the complement system, which is essential in inflammation and in the innate immune response to infection¹³. Complement’s wide-ranging activities link the innate immune response to the subsequent activation of adaptive immunity¹⁴. Circulating complement proteins are activated by cleavage, and some of the resultant products are deposited on pathogen or host cell surfaces, whereas others are released into

body fluids, where they interact with specific receptors on various target cells. Of these complement components, the C3 protein is considered central to the complement cascade. Enzymatic cleavage of C3 leads to production of the anaphylatoxin C3a, an inflammatory mediator and chemoattractant, and C3b¹⁵. C3b is involved in the opsonization and subsequent clearance of pathogens but is also a main component of the C5 convertase, an enzyme complex that cleaves C5 to produce C5a and C5b. The ensuing deposition of the C5b fragment on the cell surface contributes to the formation of the pore-like membrane attack complex (MAC) in cellular membranes, whereas the anaphylatoxin C5a is released and acts as an even more potent chemoattractant and inflammatory mediator than C3a^{13,16}.

Formation of the MAC leads to the lysis of bacteria or other foreign cells and, in certain pathophysiological conditions, to the lysis of host cells as well¹³. Given that several complement components have been found to be deposited in the tumor tissue of patients, the MAC was originally thought to contribute to the immunosurveillance of malignant tumors by complement^{17,18}. Further studies have shown, however, that malignant tumor cells are protected from such complement-mediated lysis because they overexpress complement regulators that limit complement activation and deposition *in situ* and, therefore, formation of the MAC^{17,19}. It has been postulated that the ability of the MAC to lyse foreign and host cells might enhance the efficacy of cancer immunotherapies involving monoclonal antibodies (mAbs) specific for particular tumor antigens, as complement proteins enhance antibody-dependent cytotoxicity^{20,21}.

¹Department of Pathology and Laboratory Medicine, Medical School of the University of Pennsylvania, Philadelphia, Pennsylvania 19104, USA. ²Center for Research on Reproduction and Women’s Health, Department of Obstetrics and Gynecology, University of Pennsylvania, Philadelphia, Pennsylvania 19104, USA. ³Pulmonary Division, Children’s Hospital, Boston, Massachusetts 02215, USA. ⁴Present address: Department of Biomedical Sciences, College of Osteopathic Medicine and Biomedical Engineering Program, Russ College of Engineering and Technology, University of Ohio, Athens, Ohio 45701, USA. Correspondence should be addressed to J.D.L. (lambris@upenn.edu).

Received 28 March; accepted 15 August; published online 28 September 2008; doi:10.1038/ni.1655

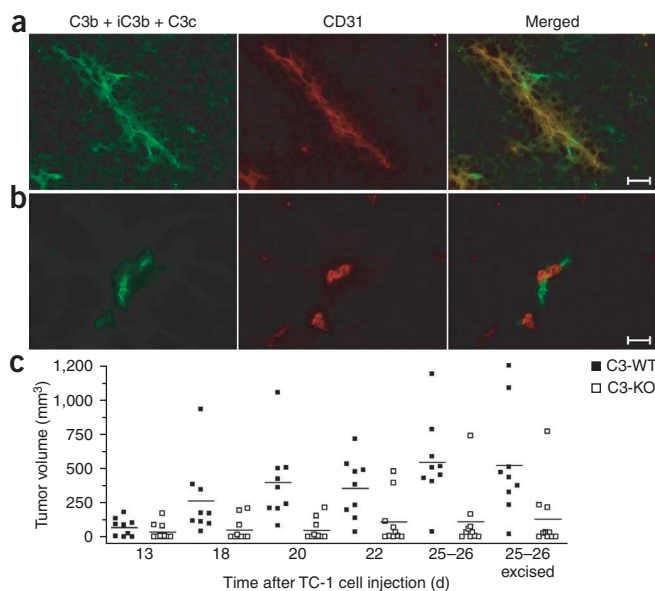


Figure 1 Complement activation is involved in tumor growth.

(a,b) Immunofluorescence detection of complement cleavage products with anti-C3 (left; green fluorescence) and of endothelial cells with anti-CD31 (middle; red fluorescence) in frozen sections of an end-point tumor (a) or surrounding benign tissue (b) from a wild-type mouse. Merged images (right) show localization of complement cleavage products in the vasculature (yellow fluorescence) or in its close proximity (green fluorescence). Scale bars, 10 μ m. Images are representative of three experiments with at least three wild-type mice. (c) Tumor volumes of C3-deficient mice (C3-KO) and littermate wild-type control mice (C3-WT) measured on various days after tumor cell injection. Far right (25–26 excised), volumes based on measurements obtained after mice were killed and tumors were removed. Each symbol represents an individual mouse; small horizontal lines indicate the mean. $P < 0.0001$ (two-way ANOVA). Data are representative of three independent experiments with ten mice per cohort in each.

Despite extensive investigation into the anticancer potential of the complement system, a distinctly different function for complement effectors as factors that might promote tumor growth has not yet been explored. Given that complement effectors such as anaphylatoxins have strong proinflammatory properties¹³ and that several inflammatory mediators favor tumor growth^{3,5,6}, we hypothesized that complement effector proteins might also promote tumor development. Using a syngeneic mouse model of tumor growth²², we show here that various complement deficiencies were associated with impaired tumor enlargement and that pharmacological blockade of the C5a receptor (C5aR; A000037) with a peptidic C5aR antagonist was able to retard tumor growth. Notably, this inhibition of C5aR signaling was associated with a considerably enhanced CD8⁺ T cell antitumor response. The strong immune response was also associated with inhibition of the recruitment of MDSCs into tumors of mice lacking C5aR signaling. In addition, MDSCs isolated from mice deficient in C5aR were less able to inhibit T cell proliferation *in vitro*. The lower capacity of C5aR-deficient MDSCs to inhibit the antigen-specific CD8⁺ T cell-mediated immune response was associated with less production of ROS and RNS by these cells. Thus, our studies demonstrate involvement of the complement anaphylatoxin C5a in promoting the growth of malignant tumors through the recruitment of MDSCs into tumors and regulating their functional capacity. Our findings indicate a new and potentially promising therapeutic application of complement inhibition to the treatment of malignant tumors.

RESULTS

Deposition of C3 fragments in engrafted tumors

Many of the functions of complement are mediated by complement effectors, such as C3a, C5a and the MAC, that are generated during the process of complement activation. We hypothesized that such complement effectors are similarly generated during tumor development. To test our hypothesis, we used the TC-1 syngeneic model of cervical cancer in mice. In this model, flank tumors rapidly develop after subcutaneous injection of cancer cells. We monitored the activation of complement in these tumor-engrafted mice by immunofluorescence staining, which showed that C3 cleavage products were extensively deposited along the tumor vasculature in wild-type mice (Fig. 1a). As expected, there was no staining in tumors from

C3-deficient mice (data not shown), whereas in benign tissue surrounding tumors in wild-type mice, only scattered C3 deposits were visible (Fig. 1b). C3 is the main protein of the complement-activation cascade, at which most of the known pathways of complement activation converge²³. Therefore, the cleavage of C3, as demonstrated by the presence of its cleavage products in tumor tissue, suggested that activation of complement proteins had occurred in these tumor-bearing mice and had led to the generation of complement effectors. However, with the assays available, we did not find substantially higher concentrations of circulating C3 cleavage fragments in the plasma of these mice (data not shown). These data indicate a local and limited activation of complement in the tumor microenvironment rather than systemic complement activation, which emphasizes the specificity of this phenomenon for tumors.

Inhibition of tumor growth by C3 deficiency

Because the formation of C3 convertase is the point in the complement cascade at which the three known pathways of complement activation converge, the elimination of C3 prevents the generation of complement effectors¹³; similarly, C3 deficiency eliminates a wide range of activities that are mediated by these effectors. As we had detected the deposition of C3 cleavage products in the microenvironment of TC-1 tumors, we assessed tumor growth in C3-deficient mice and their littermate controls after subcutaneous inoculation with TC-1 tumor cells. These experiments showed that tumor growth was significantly impaired in the absence of C3 (Fig. 1c). Tumor volumes measured at various times after subcutaneous inoculation of tumor cells were significantly lower in the C3-deficient mice than in the wild-type littermate controls over the course of the experiment. The absence of the deposition of C3 cleavage products in tumor tissue from C3-deficient mice demonstrated that the injected TC-1 cells were not producing C3 to reconstitute this deficiency. In addition, we monitored the concentrations of C3 in serum from C3-deficient and control mice throughout the experiment. None of the C3-deficient mice had a detectable concentration of C3 in their serum, nor was there an increase in C3 in the wild-type control mice over the course of the experiment, as determined by enzyme-linked immunosorbent assay (data not shown). Thus, the impairment of tumor growth in mice lacking C3 suggests that complement and complement activation are intimately involved in this process.

Complement-activation pathways in tumors

To elucidate the mechanisms of complement activation (classical, lectin and/or alternative pathways) in TC-1 tumors, we assessed tumor growth in mice deficient in complement protein C4 or complement factor B, as well as in their littermate controls, after

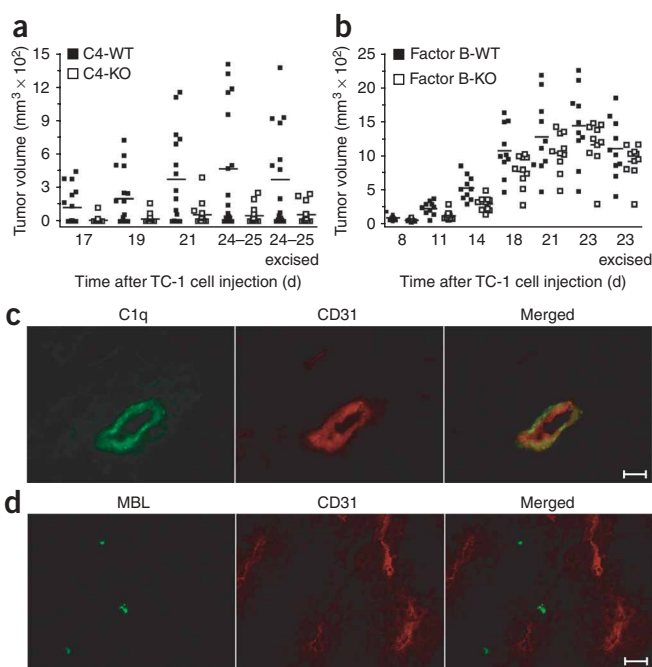


Figure 2 Involvement of the classical pathway in the activation of complement during tumor growth. **(a)** Tumor volumes of C4-deficient mice (C4-KO) and littermate wild-type control mice (C4-WT) after tumor cell injection. $P < 0.0001$ (two-way ANOVA). Data are representative of two independent experiments each with at least 12 mice per cohort. **(b)** Tumor volumes of factor B-deficient mice (Factor B-KO) and littermate wild-type controls (Factor B-WT) after tumor cell injection. $P = 0.6126$ (two-way ANOVA). Data are representative of one experiment ($n = 10$ mice per cohort). Far right (24–25 excised **(a)** or 23 excised **(b)**), excised tumors. Each symbol represents an individual mouse; small horizontal lines indicate the mean **(a,b)**. **(c)** Immunofluorescence detection of C1q with anti-C1q (left; green fluorescence) and of endothelial cells with anti-CD31 (middle; red fluorescence) in frozen sections of an end-point tumor from a wild-type mouse. Merged image (right) shows localization of C1q in the vasculature (yellow fluorescence). **(d)** Staining as described in **c** but with antibody to mannan-binding lectin (MBL; left; green fluorescence) instead of anti-C1q. Merged image; right. Scale bars **(c,d)**, 10 μm . Images **(c,d)** are representative of two experiments with at least five wild-type mice.

characteristic of C3 deposits, we concluded that this pathway is the main contributor to complement activation in engrafted tumors. The functional relevance of the lectin pathway for complement activation in engrafted tumors remains to be established.

Inhibition of C5aR impairs tumor growth

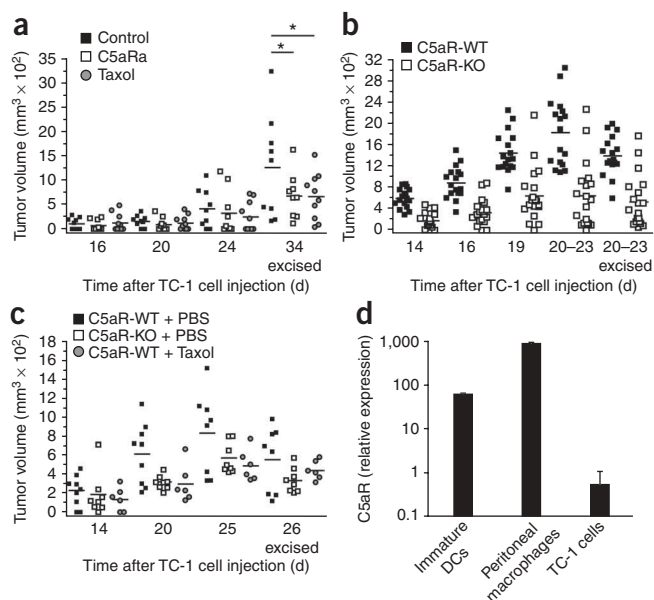
The C5a anaphylatoxin activates several cellular responses involved in tumor growth and progression, including the expression of adhesion molecules on endothelial cells and the release of various cytokines from leukocytes²⁴. These properties of C5a and the results obtained from our study of C3-deficient mice prompted us to investigate whether C5a is required for tumor growth in our model. For this, we blocked C5aR in tumor-bearing wild-type mice with a C5aR antagonist, the hexapeptide AcF(OP(D)ChaWR)²⁵, beginning treatment 1 week after the injection of tumor cells.

The pharmacological blockade of the C5aR with this antagonist resulted in impaired tumor growth in the antagonist-treated mice relative to that in control mice treated with PBS (**Fig. 3a**). To estimate whether the therapeutic effectiveness of the C5aR antagonist in retarding tumor growth was similar to the effects achieved by the treatment of tumor-bearing mice with broadly used anticancer drugs,

subcutaneous inoculation with TC-1 tumor cells. C4 deficiency resulted in much less tumor growth (**Fig. 2a**). Given that C4 is required for the formation of the classical or lectin pathway C3 convertases, that result suggested a contribution by one of those pathways to complement activation and subsequent C3 cleavage in engrafted tumors. Deficiency in factor B had no substantial effect on tumor growth (**Fig. 2b**), which ruled out the possibility of any large contribution from the alternative pathway, as factor B is an essential component of the alternative-pathway C3 convertase.

To determine whether the classical or lectin pathway is involved in complement activation in tumor tissue, we evaluated TC-1 tumors from wild-type mice for the deposition of complement proteins that initiate those pathways. We found moderate deposits of complement protein C1q along tumor vasculature (**Fig. 2c**), whereas deposition of mannan-binding lectin did not have a distinct association with tumor blood vessels (**Fig. 2d**). As C1q initiates the classical pathway of complement activation and C1q deposition followed the pattern

Figure 3 Lack of C5aR signaling decreases tumor growth with efficiency similar to that of paclitaxel treatment. **(a)** Tumor volumes of wild-type mice treated with the C5aR antagonist (C5aRa), paclitaxel (Taxol) or PBS (Control). *, $P < 0.05$ (two-way ANOVA, Bonferroni post-test). Data are representative of two independent experiments ($n_1 \geq 9$ mice per cohort; $n_2 = 5$ mice per cohort). **(b)** Tumor volumes of C5aR-deficient mice (C5aR-KO) and littermate wild-type control mice (C5aR-WT). $P < 0.0001$ (two-way ANOVA). Data are representative of one experiment ($n \geq 17$ mice per cohort). **(c)** Tumor volumes of C5aR-wild-type mice treated with PBS or paclitaxel, and of C5aR-deficient mice treated with PBS. $P = 0.004$ (two-way ANOVA). Data are representative of one experiment ($n \geq 6$ mice per cohort). Far right (34 excised **(a)**, 20–23 excised **(b)**, and 26 excised **(c)**), excised tumors. Each symbol represents an individual mouse; small horizontal lines indicate the mean **(a–c)**. **(d)** C5aR expression in TC-1 cells, immature dendritic cells (DCs) and peritoneal macrophages, presented as the ratio of C5aR mRNA to 1×10^4 GAPDH mRNA molecules. C5aR was considered present if more than five copies of mRNA were detected for every 1×10^4 copies of GAPDH mRNA. Data are representative of three independent experiments.



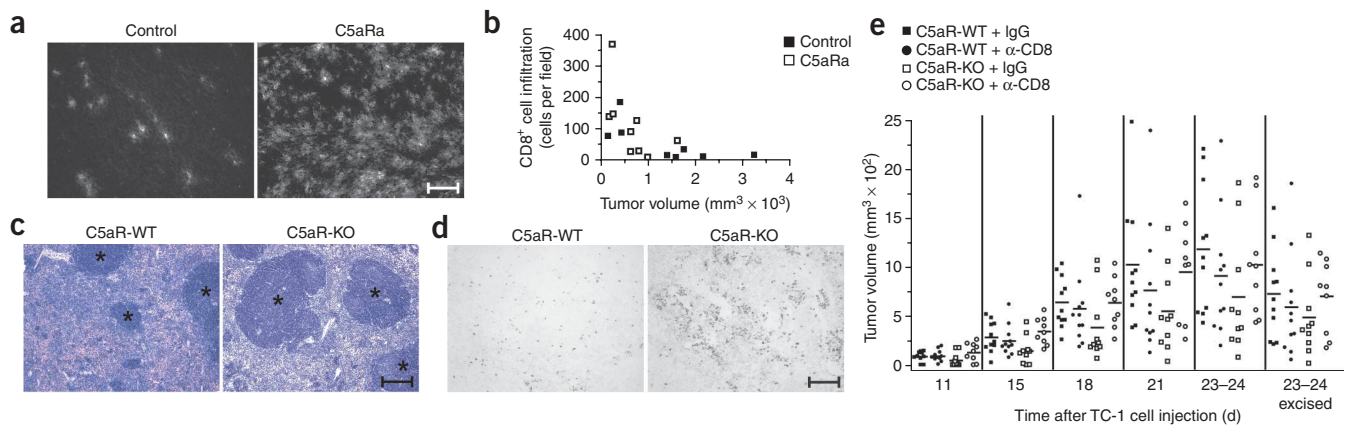


Figure 4 The antitumor T cell response is enhanced in mice lacking C5aR signaling. **(a)** Infiltration of end-point tumor tissue with CD8⁺ T cells in a control mouse (left) and a mouse treated with the C5aR antagonist. Fluorescence indicates CD8 expression on infiltrating T cells. Scale bar, 30 μm . Images are representative of one experiment ($n \geq 8$ mice per cohort). **(b)** Tumor-infiltrating CD8⁺ T cells versus tumor volume, based on the immunofluorescence studies in **a** and presented as cells counted per 200 \times field. $P = 0.0180$ and $r = -0.5653$ (Pearson correlation). Data are representative of one experiment ($n \geq 8$ mice per cohort). **(c)** Hematoxylin and eosin-stained sections of end-point spleens from a tumor-bearing C5aR-deficient mouse (right) and a tumor-bearing littermate wild-type mouse (left). *, areas of white pulp. Scale bars **(c,d)**, 60 μm . Images **(c,d)** are representative of one experiment ($n \geq 9$ mice per cohort). **(d)** BrdU⁺ end-point splenocytes in a C5aR-wild-type mouse (left) and a C5aR-deficient mouse (right) bearing tumors. Scale bars **(c,d)**, 60 μm . Images **(c,d)** are representative of one experiment ($n \geq 9$ mice per cohort). **(e)** Tumor volumes of C5aR-deficient and C5aR-wild-type mice treated with IgG or anti-CD8 (α -CD8). Far right (23–24 excised), excised tumors. Each symbol represents an individual mouse; small horizontal lines indicate the mean. $P = 0.0003$, C5aR-wild-type plus IgG versus C5aR-deficient plus IgG; $P = 0.0006$, C5aR-deficient plus IgG versus C5aR-deficient plus anti-CD8 (two-way ANOVA). Data are representative of one experiment ($n \geq 9$ mice per cohort).

we also assessed tumor volumes in wild-type mice treated with the established anticancer drug paclitaxel alone at a dose shown before to suppress tumor growth²⁶. Comparison of the tumor volumes of mice treated with the C5aR antagonist and those treated with paclitaxel showed that inhibition of tumor growth by the complement inhibitor was similar to that achieved by treatment with this anticancer therapeutic (Fig. 3a).

We further confirmed the specificity of our findings by assessing tumor growth in mice deficient in C5aR. Consistent with our hypothesis and the results obtained with mice treated with the C5aR antagonist, these C5aR-deficient mice had significantly lower tumor volumes than those of their littermate controls (Fig. 3b). Furthermore, we found that the suppressive effect of genetic C5aR deficiency on tumor growth was similar to that obtained by treating wild-type mice with paclitaxel (Fig. 3c), which indicated that lack of C5aR inhibits tumor growth as well as an established anticancer drug does. These experiments also suggested that C5aR expressed on host cells is involved in the regulation of tumor growth. We initially noted that C5aR mRNA was not present in TC-1 cells in culture (Fig. 3d), but we could not exclude the possibility that C5aR is upregulated in tumor cells *in vivo*. However, if C5aR signaling on TC-1 cells contributed to tumor growth, these cells should still have grown in C5aR-deficient mice, as only the host cells lacked the ability to express C5aR in these mice. Therefore, these experiments suggest that C5a contributes to the control of tumor growth by acting mainly on receptors expressed by host cells, regardless of their expression on tumor cells.

To exclude the possibility that the effect of the C5aR antagonist on tumor growth was related to nonspecific cytotoxicity of this peptide toward tumor cells, we evaluated whether treating C5aR-deficient mice with the C5aR antagonist further delayed tumor growth. We also used the control peptide AcF(OP(D)ChaA(D)R), which has the same length as and physicochemical properties similar to those of the C5aR antagonist but does not have the ability to block C5aR signaling^{25,27}. By using this control peptide, we aimed to determine

whether alteration of the cellular microenvironment by injected peptides, rather than their biological activity, influenced the rate of tumor growth.

The treatment of C5aR-deficient mice with C5aR antagonist did not induce any further inhibition of tumor growth relative to that of mice treated with control peptide (Supplementary Fig. 1 online). In addition, TC-1 tumors grew more slowly in C5aR-deficient mice than in wild-type controls regardless of the treatment of both cohorts with the control peptide (Supplementary Fig. 1). Therefore, we concluded that the effects of the C5aR antagonist on tumor growth in wild-type mice were related exclusively to the ability of this peptide to disable C5aR function.

Regulation of the antitumor immune response by C5a

To elucidate the mechanism by which C5a contributes to tumor growth, we assessed several parameters that influence tumor development (tumor cell proliferation and apoptosis, and the extent of angiogenesis) in end-point tumor specimens from mice treated with either the C5aR antagonist or PBS. There were only minimal differences between experimental groups in these parameters without statistical significance (Supplementary Fig. 2 online). This result suggests that other mechanisms, such as the elimination of tumor cells by the immune system, may contribute to the phenotype noted in mice in which C5a activity was blocked. Given the crucial function of cytotoxic T cells in controlling tumor growth, we next compared the absolute numbers of CD8⁺ cells infiltrating tumor tissue in C5aR antagonist-treated and control mice. Immunofluorescence staining showed that mice in which C5aR signaling was blocked had tumors heavily infiltrated by CD8⁺ cells, whereas in most control mice, only a few of these T cells were present in whole-tumor sections (Fig. 4a). Furthermore, quantification of the CD8⁺ infiltrates showed that there was also an inverse correlation between tumor size and the number of infiltrating CD8⁺ cells (Fig. 4b).

Those data were confirmed by our finding that the percentages of activated CD3⁺CD8⁺(CD4⁻)CD25⁺ and CD3⁺CD8⁺(CD4⁻)CD69⁺

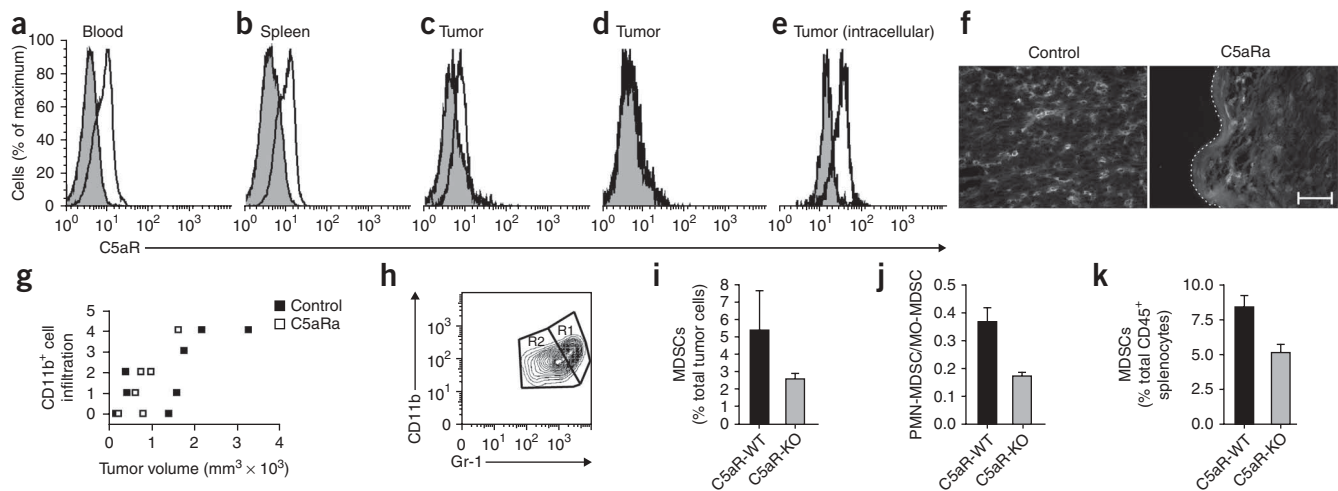


Figure 5 The migration of myeloid-derived cells into tumors is C5aR dependent. (a–e) Expression of C5aR (open histograms) versus staining with isotype-matched control antibody (shaded histograms) on MDSCs obtained from blood (a), spleen (b) and tumors (c–e) of wild-type mice. Values in e are for the cells in d made permeable before staining. (f) Infiltration of CD11b⁺ cells into tumors of a control mouse (left) and a mouse treated with the C5aR antagonist (right). White dashed line (right) indicates the tumor border. Scale bar, 30 μ m. (g) Tumor-infiltrating CD11b⁺ cells versus tumor volume, based on the assay in f. $P = 0.0003$ and $r = 0.7670$ (Pearson correlation). (h) Characteristics of CD45⁺CD11b⁺Gr-1⁺ cells from tumors from mice that were littermates of C5aR-deficient mice. R1, PMN-MDSCs; R2, MO-MDSCs. (i) MDSCs in tumors from C5aR-wild-type and C5aR-deficient mice. $P = 0.23$ (t -test). (j) Ratio of PMN-MDSCs to MO-MDSCs in total tumor MDSC populations of C5aR-wild-type and C5aR-deficient mice. $P = 0.001$ (t -test). (k) CD11b⁺Gr-1⁺ MDSCs among CD45⁺ splenocytes from C5aR-wild-type and C5aR-deficient mice. $P = 0.0024$ (t -test). Data are representative of two experiments with at least five mice per cohort (a–e) or of one experiment with eight mice (f), at least six mice (g) or sixteen mice (h–k) per cohort (mean and s.e.m., i–k).

T cells were slightly higher in tumors from C5aR-deficient mice than in those from their littermates ($n = 3$ mice per cohort), as estimated by flow cytometry ($28.7\% \pm 3.4\%$ versus $21.1\% \pm 1.8\%$ for CD25⁺ and $24.4\% \pm 3.2\%$ versus $16.7\% \pm 2.2\%$ for CD69⁺, respectively). However, these differences did not reach statistical significance. Finally, we found that the white pulp follicles in the spleen were larger and the proliferation of lymphoid cells in these structures was higher in C5aR-deficient mice bearing tumors than in their tumor-bearing littermate controls (Fig. 4c,d).

The results reported above suggested that C5a modulates the CD8⁺ T cell-mediated antitumor immune response. Therefore, we hypothesized that the slower tumor growth in C5aR-deficient mice and in wild-type mice treated with C5aR antagonist was a result of the infiltration of these tumors by CD8⁺ T cells. To confirm our hypothesis, we did experiments in which we depleted C5aR-deficient and control mice of CD8⁺ T cells by treating them with CD8-specific antibody followed by inoculation with tumor cells. We expected that this depletion in C5aR-deficient mice would result in a higher rate of tumor growth. Indeed, even the partial elimination of these cells from C5aR-deficient mice accelerated tumor growth in these mice to the rate of tumor growth in wild-type controls (Fig. 4e). Depletion of CD8⁺ T cells did not affect tumor growth in wild-type controls. That result was also expected on the basis of the finding that only a few CD8⁺ T cells infiltrated tumors in untreated wild-type mice (Fig. 4a). Preliminary experiments with mice not bearing tumors showed that injection of antibody to CD8 (anti-CD8) at a dose selected to deplete CD8⁺ T cells resulted in more than 95% depletion of CD8⁺ T cells (data not shown). However, monitoring of the peripheral blood and spleens of mice bearing tumors showed that by injecting anti-CD8, we achieved only partial depletion of CD8⁺ T cells in these mice (Supplementary Fig. 3a,b online). Notably, however, the degree of CD8⁺ T cell depletion strongly and positively correlated with the rate of tumor growth in C5aR-deficient mice (Supplementary Fig. 3c,d). This positive correlation confirmed that the acceleration of tumor

growth in C5aR-deficient mice that had been injected with anti-CD8 was a result of CD8⁺ T cell depletion. Furthermore, tumors from C5aR-deficient mice treated with anti-CD8 had fewer CD8⁺ T cells than did tumors from C5aR-deficient mice treated with control rat immunoglobulin G (IgG), as demonstrated by immunofluorescence analysis (Supplementary Fig. 3e).

Regulation of MDSC accumulation and migration by C5a

Our observations suggested that C5a signaling contributes to the inhibition of the immune response to tumor cells. Cells of myeloid origin, including MDSCs and tumor-associated macrophages, have been shown to be important for suppression of the immune response to tumor antigens and promotion of tumor growth in mice and humans. In addition, it is well known that granulocytes, monocytes and tissue macrophages, which are the mature counterparts of MDSCs, have abundant expression of C5aR¹⁶. Moreover, we found that complement proteins were deposited in tumor tissue (Fig. 1a), which suggested the occurrence of local complement activation with the concomitant generation of C5a. Therefore, we hypothesized that C5a might contribute to the inhibitory properties of MDSCs.

Our initial studies showed that CD45⁺CD11b⁺Gr-1⁺ MDSCs isolated from the spleen and blood of naive mice expressed C5aR to an extent similar to that of mature granulocytes and monocytes (Supplementary Fig. 4a,b online). Similarly, we found C5aR expression on the surface of MDSCs circulating in the peripheral blood (Fig. 5a) or residing in the spleen (Fig. 5b) of tumor-bearing mice. The expression of C5aR was lower on the surface of tumor-associated MDSCs (Fig. 5c) than on MDSCs in the peripheral blood and spleen. Unexpectedly, MDSCs isolated from the tumors of some wild-type mice did not have any surface expression of C5aR (Fig. 5d). However, when MDSCs from the same tumors were made permeable before staining, C5aR was detectable in the cytoplasm (Fig. 5e). This result showed that C5aR was internalized in tumor-associated MDSCs. The

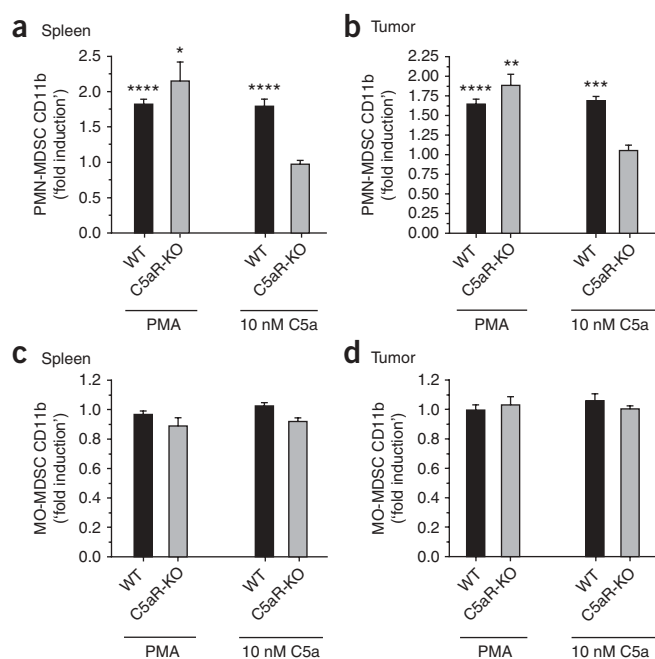


Figure 6 C5a upregulates CD11b expression in PMN-MDSCs. Flow cytometry of the induction of CD11b expression on PMN-MDSCs (a,b) and MO-MDSCs (c,d) from the spleens (a,c) and tumors (b,d) of wild-type mice and C5aR-deficient mice, after treatment of cells with PMA or 10 nM C5a. Results are presented as expression in stimulated cells relative to baseline expression in unstimulated cells from the same mice (set as 1). *, $P = 0.0232$; **, $P = 0.0040$; ***, $P = 0.0003$; ****, $P < 0.0001$, stimulated versus unstimulated (one-sample t -test). Data are representative of one experiment (mean and s.e.m. of five or more mice per cohort).

mechanisms apply to MDSCs migrating to tumor tissue. As CD11b is the α_M subunit of the integrin CR3, which interacts with the $\alpha_L\beta_2$ integrin ligand ICAM-1 expressed on endothelial cells during leukocyte extravasation, we obtained MDSCs from tumors and spleens and evaluated the changes in CD11b expression after we stimulated the cells with C5a *in vitro*. Wild-type PMN-MDSCs isolated from spleens and tumors had significantly higher expression of CD11b after C5a stimulation by upregulating CD11b (Fig. 6a,b), whereas MO-MDSCs did not respond to C5a stimulation by upregulating CD11b (Fig. 6c,d), in agreement with published findings showing that C5a stimulates CD11b expression in neutrophils²⁹. These results supported our hypothesis that C5a contributes to the recruitment of PMN-MDSCs to tumors. The specificity of these findings was confirmed by the lack of CD11b upregulation in C5aR-deficient MDSCs stimulated with C5a (Fig. 6), despite the response of these cells to phorbol myristate acetate (PMA; Fig. 6a,b,d), which we used as a positive control to assess the ability of MDSCs to respond to *in vitro* stimuli.

Modulation of ROS and RNS production in MDSCs by C5a

We next analyzed the capacity of Gr-1⁺ MDSCs isolated from tumors obtained from C5aR-deficient mice and C5aR-sufficient mice to inhibit the proliferation of CD3⁺ T cells originating from the spleens of naive mice. MDSCs recovered from the tumor microenvironment of C5aR-deficient mice had either a total inability or a lower capacity to inhibit phytohemagglutinin-induced T cell proliferation than did MDSCs from the tumors of littermate control mice (Fig. 7a). These observations suggest that C5a contributes not only to the migration of MDSCs into tumors but also to their functional capacity to inhibit the T cell response to tumor cells.

Given that MDSCs are known to inhibit the antitumor antigen-specific CD8⁺ T cell response by producing large amounts of highly suppressive ROS and RNS¹¹ and that C5a is involved in regulating the synthesis of ROS and RNS in macrophages³⁰ and neutrophils³¹, which are thought to be the mature counterparts of MDSCs, we hypothesized that C5a influences the suppressive ability of MDSCs by regulating their production of ROS and RNS. As demonstrated by flow cytometry, the overall amount of ROS and RNS in MDSCs isolated from tumors from C5aR-deficient mice was much lower than that in MDSCs from tumors from wild-type controls (Fig. 7b,c). As we had found that C5a influenced the ratio of MO-MDSCs to PMN-MDSCs (Fig. 5j), we analyzed the contribution of each subpopulation to the production of ROS and RNS. We found that in both C5aR-deficient and C5aR-sufficient mice, tumor-associated PMN-MDSCs produced significantly more ROS and RNS than did the corresponding MO-MDSCs (Fig. 7d). However, when comparing PMN-MDSCs in C5aR-deficient and C5aR-sufficient mice, we did not find a difference in the production of ROS and RNS (Fig. 7d). Conversely, MO-MDSCs from tumors growing in C5aR-deficient mice synthesized less ROS and RNS than did their wild-type counterparts (Fig. 7d). Therefore, it seems that C5a augments the production of ROS and RNS only in MO-MDSCs. However, given that C5a increases the migration of ROS- and RNS-rich PMN-MDSCs into the

rapid internalization most G protein-coupled receptors occurs as a regulatory mechanism in response to the constant presence of ligands.

As C5a is known to be a strong chemoattractant¹⁶, we investigated the involvement of C5a in the migration of cells of myeloid origin into tumors. Immunofluorescence staining of tumor sections showed that mice treated with the C5aR antagonist had fewer cells expressing CD11b than did mice treated with PBS (Fig. 5f). Notably, CD11b⁺ cells in mice treated with C5aR antagonist were located only at the periphery of the tumors, whereas in control mice they were present throughout the tumor sections. We also found a positive correlation between the number of CD11b⁺ cells and tumor volume in both experimental groups (Fig. 5g).

Flow cytometry of CD45⁺CD11b⁺Gr-1⁺ cells isolated from tumors from C5aR-deficient and control mice showed the presence of two distinct subpopulations of MDSCs that differed in the extent of their expression of CD11b and Gr-1 (Fig. 5h). These subpopulations corresponded to mononuclear MDSCs (MO-MDSCs) and polymorphonuclear MDSCs (PMN-MDSCs), which have been described before²⁸. PMN-MDSCs were characterized by higher expression of both CD11b and Gr-1 (Fig. 5h, R1) than that of MO-MDSCs (Fig. 5h, R2). Although the percentage of total MDSCs isolated from tumors from wild-type mice was higher than the percentage of these cells in tumors from C5aR-deficient mice, this difference did not reach statistical significance (Fig. 5i). However, we noted that the ratio of PMN-MDSCs to MO-MDSCs was significantly higher in tumors from wild-type mice than in tumors from C5aR-deficient mice (Fig. 5j). Therefore, we concluded that C5a influences mainly the migration of PMN-MDSCs into tumors. In addition, the percentage of CD11b⁺Gr-1⁺ MDSCs in the CD45⁺ cell population isolated from the spleens of wild-type mice was higher than the percentage of these cells in the spleens of C5aR-deficient mice (Fig. 5k). This observation suggests that C5a is involved in the processes of MDSC migration and accumulation in peripheral lymphoid organs.

The migration of PMN-MDSCs to tumors requires they cross the endothelial barrier. To leave the circulation and migrate to interstitial tissues, leukocytes require interaction of their integrins with adhesion molecules on endothelial cells. We hypothesized that the same

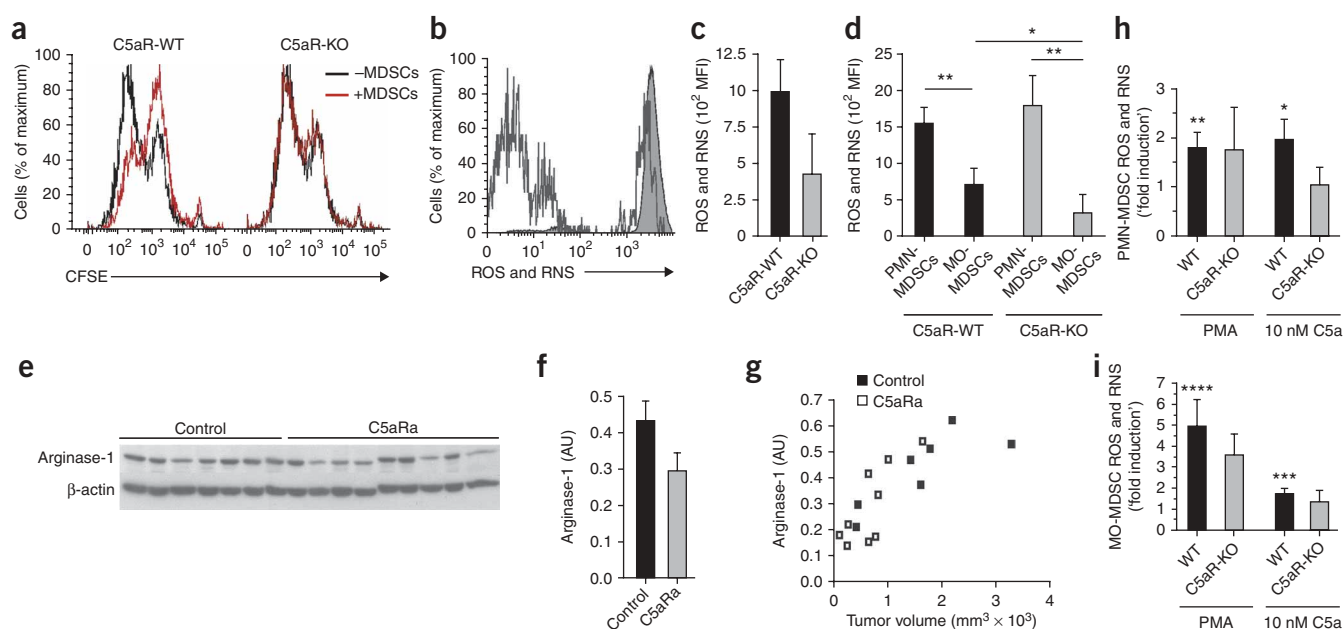


Figure 7 C5a enhances the suppressive capacity of tumor-associated MDSCs by regulating the production of ROS and RNS. **(a)** Phytohemagglutinin-induced proliferation of CD3⁺ splenocytes from non-tumor-bearing wild-type mice in the presence (+) or absence (–) of Gr-1⁺ MDSCs from tumors from C5aR–wild-type or C5aR-deficient mice. **(b)** Production of ROS and RNS in MDSCs from tumors from C5aR–wild-type mice (shaded histogram) and C5aR-deficient mice (open histogram). **(c)** Quantification of the production of ROS and RNS by MDSCs from tumors from C5aR–wild-type and C5aR-deficient mice. $P = 0.0210$ (Wilcoxon). **(d)** Quantification of the production of ROS and RNS by PMN-MDSCs and MO-MDSCs from tumors of C5aR–wild-type and C5aR-deficient mice. *, $P = 0.0342$; **, $P = 0.0005$ (Wilcoxon). MFI, median fluorescence intensity. **(e)** Arginase-1 expression in tumors from PBS-treated control mice and C5aR antagonist-treated mice. **(f)** Quantification of the immunoblot in **e**. $P = 0.0844$ (*t*-test). **(g)** Correlation between arginase-1 expression (**f**) and tumor volumes. $P = 0.0256$ and $r = 0.8147$, control; $P = 0.0105$, $r = 0.7947$, C5aR antagonist (Pearson correlation). AU, arbitrary units. **(h)** Induction of ROS and RNS in PMN-MDSCs (**h**) and MO-MDSCs (**i**) from the spleens of wild-type and C5aR-deficient mice, after treatment of cells with PMA or 10 nM C5a. Results are presented as ROS in stimulated cells relative to baseline in unstimulated cells from the same mice. *, $P = 0.0382$; **, $P = 0.0270$; ***, $P = 0.0245$; ****, $P < 0.0092$ stimulated versus unstimulated (one-sample *t*-test). Data are representative of one experiment with three mice per cohort (**a**), 12 or more mice per cohort (**b–d**), seven or more mice per cohort (**e–g**) or five or more mice per cohort (**h,i**; mean and s.e.m., **c,d,f,h,i**).

tumor, large amounts of ROS and RNS in the tumor microenvironment of wild-type mice is a net effect of dual C5a activity. C5a induces the migration of highly suppressive, ROS- and RNS-rich PMN-MDSCs into the tumor microenvironment; additionally, it increases the production of ROS and RNS by MO-MDSCs.

Arginase-1 activity is essential for the immunosuppressive abilities of MDSCs and contributes to the production of ROS and RNS by these cells¹². Therefore, we analyzed the expression of this enzyme in whole-cell extracts of tumors from mice treated with C5aR antagonist and in control mice (**Fig. 7e**). Arginase-1 expression was only slightly lower in mice treated with C5aR antagonist, without reaching statistical significance (**Fig. 7f**). However, we noted a strong significant positive correlation between arginase-1 expression and tumor volume (**Fig. 7g**) in both groups, with a correlation coefficient (Pearson *r*) of 0.802.

To further confirm the results of the *in vivo* studies reported above, we stimulated MDSCs from spleens and tumors of wild-type mice to produce ROS and RNS by incubating them with various concentrations of C5a *in vitro*. We used MDSCs isolated from C5aR-deficient mice as an additional control in these experiments. Both subpopulations of MDSCs isolated from spleens responded to C5a stimulation with higher production of ROS and RNS than of unstimulated cells obtained from the same mouse (**Fig. 7h,i**). As expected, MDSCs from spleens of C5aR-deficient mice did not respond to C5a stimulation, despite their brisk response to PMA stimulation (**Fig. 7h,i**). Tumor-associated MDSCs did not respond to C5a stimulation, regardless of which subpopulation of MDSCs was analyzed (data not shown). We

concluded that the unresponsiveness of tumor-associated MDSCs to *in vitro* C5a stimulation was a result of strong stimulation of these cells for the production of ROS and RNS *in vivo* in the tumor microenvironment and exhaustion of this system; therefore, further stimulation of these cells *in vitro* failed. That conclusion was supported by the finding of much more initial production of ROS and RNS in tumor-associated MDSCs than in MDSCs obtained from spleens (data not shown) and the lack of an increase in the production of ROS and RNS in tumor-associated MDSCs in response to PMA stimulation (data not shown).

DISCUSSION

Interest in complement as a potential anticancer effector system has been revived in the context of anticancer therapies with mAbs to tumor cell antigens. Several studies have indicated that blocking or overriding complement-regulatory proteins might substantially improve the efficacy of anticancer mAb immunotherapy²⁰. However, despite the large number of studies dedicated to assessing the contribution of complement to cancer pathogenesis and therapy, none of these investigations has addressed the possible involvement of the complement effectors in promoting the growth of malignant tumors. This gap in the understanding of the function of complement in cancer is unexpected, given that complement effectors, in particular C5a, are potent proinflammatory mediators and that inflammation and infection are widely understood to be able to both promote and exacerbate tumor growth. The only recent study investigating whether C3 promotes tumor formation involved the development of dysplastic

intraepithelial lesions in a model of multistage epithelial carcinogenesis (HPV16 mice). However, that study has shown that the activation of complement does not contribute to the recruitment of inflammatory cells, the induction of keratinocyte hyperproliferation or the activation of angiogenesis during the development of epidermal dysplasia³². Direct comparison of those results with our data is difficult, as the model used in that investigation assessed the contribution of complement exclusively in premalignant skin lesions, whereas here we have studied the function of complement in advanced, invasive tumors.

The results of our study suggest that the complement system indeed contributes to mechanisms that promote the growth of malignant tumors. Using a mouse model of tumor growth in which we inoculated TC-1 malignant cells subcutaneously into mice, we have shown that deficiency in C3, C4 or C5aR is associated with retardation of tumor growth. In addition, pharmacological blockade of the C5aR with a peptidic C5aR antagonist also decreased tumor growth. The effects of treatment of wild-type mice with the C5aR antagonist were similar to those of the anticancer drug paclitaxel administered to mice at one sixth the lethal dose. Notably, the dose of paclitaxel we used here was several times higher than the therapeutic dose used for human patients with cancer (20 mg per kg body weight per week versus 3.3–4.3 mg per kg body weight every 3 weeks for the treatment of ovarian cancer, according to the results of clinical studies provided by the manufacturer). These experiments collectively suggest that C5aR signaling promotes the growth of TC-1 tumors.

In most cases, the activation of C5 requires prior activation of C3 (ref. 23). However, in specific pathophysiological conditions, C5a can be generated in the absence of C3 (ref. 33). The similar degree of inhibition of tumor growth we noted in C3-deficient, C5aR-deficient and C5aR antagonist-treated mice suggested that in our experimental model, C5 activation required prior cleavage of C3 through complement activation. Furthermore, the presence of C3 cleavage products in tumor tissue indicated that C5a was generated locally in the tumor microenvironment and subsequently contributed to mechanisms supporting tumor growth. The impairment of tumor growth in C4-deficient mice together with the local deposition of C1q in tumor tissue indicated involvement of the classical pathway in the activation of complement during tumor development. Also, the lower growth of tumors in C5aR-deficient mice suggested that a C5a-mediated tumor-promoting activity was most relevant to host cells, because the lack of C5aR signaling was limited to those cells in our experimental conditions.

The enhanced infiltration of tumors by CD8⁺ T cells we noted in mice with blocked C5aR activity indicated the possibility that C5a has an immunomodulatory function in tumor growth. Several studies with animal experimental models, as well as studies in humans, have demonstrated a crucial function for cytotoxic CD8⁺ T cells in adaptive immunity to tumors^{2,34,35}. Therefore, given that blocking C5aR enhanced the CD8⁺ T cell response in the tumor microenvironment in our model, we hypothesize that C5a promotes the growth of TC-1 tumors by suppressing the adaptive immune response to tumor antigens. That conclusion was further supported by the evident abrogation of the effect of C5aR deficiency on the growth of tumors by depletion of CD8⁺ T cells in these mice. Although modulation of the adaptive immune response to tumors by complement is an as-yet-unexplored area, several studies have shown that complement anaphylatoxins regulate adaptive immune responses at many levels^{36–39}, particularly in models of allergic disorders^{40,41}. Notably, despite its proallergic properties in an inflamed environment, C5a regulates tolerance to inhaled antigens in the respiratory tract. C5aR signaling

affects the function of pulmonary dendritic cells and regulatory T cells, which leads to suppression of the immune response to airborne antigens^{40,42,43}. These immunosuppressive functions of C5a in the respiratory tract support our hypothesis that C5a might have similar abilities in mice bearing tumors.

One of the important mechanisms used by malignant tumors to suppress the immune response to tumor antigens is abnormal myelopoiesis and the recruitment of myelomonocytic cells to the tumor site and peripheral lymphoid organs^{9,44}. MDSCs, the subset of these cells characterized by coexpression of CD11b and Gr-1 in mice, are the immature counterparts of myeloid-derived antigen-presenting cells and peripheral blood monocytes. MDSCs are able to deregulate and/or suppress T cell-dependent tumor cytotoxicity in tumor-bearing mice and in human patients with cancer⁹. Given the effects of C5a on antigen-presenting dendritic cells in the lungs and the well known chemotactic activity of this anaphylatoxin, we hypothesize that the immunosuppressive ability of C5a is associated with the C5a-mediated recruitment and/or activation of MDSCs in tumor-bearing mice. Although these cells are also present in mice without tumors, their numbers are low and they lack immunosuppressive abilities⁹.

Our initial observations indicated that C5aR expression on MDSCs was similar to its expression on peripheral blood monocytes and granulocytes, which are well known targets for the proinflammatory activities of C5a. High C5aR expression on MDSCs further supported our initial hypothesis. Indeed, tumors from mice lacking C5aR signaling showed only minimal infiltration by CD11b⁺ myeloid-derived cells, which was limited to the periphery of tumors, whereas wild-type control mice had more of these cells and a widespread distribution of these cells throughout the tumor tissue. Flow cytometry of CD11b⁺Gr-1⁺ MDSCs isolated from tumors and spleens of C5aR-deficient and control mice inoculated with TC-1 cells confirmed that C5a contributes to the accumulation of MDSCs in peripheral lymphoid organs, as well as to the migration of these cells into tumors. The peripheral localization of myeloid cells in the tumors of mice lacking C5aR signaling might also suggest that the chemotactic activity of C5a contributes to the migration of these cells throughout the tumor tissue. That hypothesis was further supported by the finding of deposition of C3 cleavage products along the tumor vasculature, which indicated that complement activation and the subsequent generation of C5a occur in tumor tissue wherever blood vessels are present.

C5a also influenced the functional properties of MDSCs, as demonstrated by the inability of isolated Gr-1⁺ cells from C5aR-deficient tumor-bearing mice to inhibit the proliferation of CD3⁺ T cells *in vitro*. That observation was confirmed by the lower proliferation of lymphoid cells in the white pulp of spleens from these mice. These data are in agreement with published findings that suppression of the T cell immune response to tumor antigens is not limited to the tumor environment but extends to the peripheral lymphoid organs, where immunosuppressive MDSCs are also present and may interact with tumor-specific cytotoxic T cells⁹.

Flow cytometry of MDSCs isolated from tumors confirmed that C5a contributes to suppression of the antitumor T cell response by regulating the amount of highly suppressive ROS and RNS in the tumor microenvironment. Notably, we found that C5a had a profound influence on the two functionally and morphologically distinct subpopulations of MDSCs, MO-MDSCs and PMN-MDSCs, that have been described before²⁸. We noted that C5a contributed to the recruitment into tumors of PMN-MDSCs, which produced much more ROS and RNS than did MO-MDSCs. In addition, C5a increased the production of ROS and RNS in MO-MDSCs. Thus, the large amount of T cell-suppressive ROS and RNS in the tumor

microenvironment is a result of both the recruitment of ROS- and RNS-rich PMN-MDSCs into tumors and upregulation of the production of ROS and RNS in MO-MDSCs by C5a.

In summary, our study has indicated a previously undefined function for complement in tumor biology. We have shown that complement activation and C5a signaling were required for the efficient recruitment of MDSCs into tumors and for the ability of these myeloid-derived cells to suppress the CD8⁺ T cell-mediated antitumor response. In addition, we have demonstrated that in our system, inhibition of complement signaling by pharmacological intervention was as efficient as the well accepted chemotherapeutic agent paclitaxel in hindering the growth of malignant tumors.

Notably, the data we have presented here were obtained from studies of a single experimental model of tumor growth. Given the enormous diversity of neoplastic diseases and the context-dependent properties of the complement system⁴⁵, extrapolation of these results to other experimental as well as clinical situations should be made carefully. Further studies are needed to extend our findings to other relevant cancer-related systems, especially in the context of the dual function of inflammation and infection in cancer pathogenesis⁴⁶. Our findings support the idea that chronic and moderate inflammation promotes tumor growth. However, it has also long been recognized that acute and brisk inflammation can induce tumor regression⁴⁶.

Our findings reported here not only introduce a new complement-mediated mechanism of tumor-dependent immunosuppression but also provide preliminary evidence of the potential utility of a therapeutic option, complement inhibition, in anticancer therapy. This perspective is particularly useful because of the relatively few side effects reported for complement-directed therapy^{47,48}, in contrast to the high toxicity associated with the anticancer chemotherapeutics in use now. Moreover, given that complement inhibition overrides tumor-dependent immunosuppression, this therapeutic approach may also hold promise as a supplement to antitumor vaccines.

METHODS

In vivo studies and reagents. All mouse experiments were approved by the Institutional Animal Care and Use Committee of the University of Pennsylvania according to guidelines of the National Institutes of Health. Mice deficient in C3, C4, factor B and C5aR used in our studies have been described^{49–52}. Mice deficient in C4 and C57BL/6 mice were from The Jackson Laboratory. Mice were backcrossed for at least nine generations onto a C57BL/6 background, and their homozygous wild-type littermates were used as controls. Mice were housed in an animal facility of the University of Pennsylvania, in a barrier, on a 12-hour light/dark cycle. Water and standard rodent diet were provided *ad libitum*.

For the establishment of TC-1 tumors, male and female mice 6–16 weeks of age were anesthetized and then were injected subcutaneously with 1×10^5 TC-1 cells in the right or left rear flank. The tumorigenic TC-1 cell line, which has been described²², was from the American Type Culture Collection (CRL-2785). Beginning about 2 weeks after cell injection, mice were anesthetized and their tumors were measured with calipers every 2–4 d until the tumor size required the mice be killed. Measurements were obtained in two dimensions (length and width) because the depth of the tumor was difficult to assess in live animals. The depth of the tumor was therefore estimated based on the smaller (width) measurement, and the volume of the tumor was calculated with the following formula: volume = (length \times width \times depth) / 2. At 1 h before mice were killed, BrdU (5-bromo-2'-deoxyuridine; Sigma) was injected intraperitoneally into mice at a single dose of 50 mg per kg body weight for further assessment of tumor or immune cell proliferation. At the time mice were killed, clinical status was assessed, the mice were anesthetized, blood was collected from the inferior vena cava (with 50 mM EDTA) and spleens and tumors were removed. Excised tumors were measured in three dimensions for an accurate volume and then were weighed. Tumors and spleens were cut into sections for cell isolation, histological examination or freezing.

For pharmacological blockade of C5aR, C57BL/6J mice were injected subcutaneously with the cyclic hexapeptide AcF(OP(D)ChaWR) acetylated phenylalanine-(ornithine-proline-(D)cyclohexylalanine-tryptophan-arginine); (C5aR antagonist), in about 400 μ l of PBS, at a dose of 1 mg per kg body weight, every 2–3 d beginning 1 week after tumor cell injection (3.3 μ mol per kg body weight per week). The C5aR antagonist was synthesized in our laboratory as described²⁵. This antagonist has been shown to specifically block C5a-mediated effects in various rodent disease models^{47,53}. Paclitaxel (Taxol; Mayne Pharma) at a dose of 20 mg per kg body weight in 400 μ l PBS was injected intraperitoneally into mice once per week (23 μ mol per kg body weight per week; dose lethal to 50% of mice tested was 128 mg per kg body weight, according to the manufacturer) beginning 1 week after tumor cell injection. Control mice in experiments using the C5aR antagonist or paclitaxel were injected subcutaneously or intraperitoneally, respectively, with about 400 μ l PBS alone or in some cases were injected subcutaneously with the cyclic hexapeptide AcF(OP(D)ChaA(D)R) (acetylated phenylalanine-(ornithine-proline-(D)cyclohexylalanine-alanine-(D)arginine)^{25,27}. The pattern of the administration of this control peptide to mice followed that described for the C5aR antagonist.

For depletion of CD8⁺ T cells, mice were injected intraperitoneally with rat mAb to mouse CD8 (53-6.72) at a dose of 200 μ g per mouse for 3 consecutive days. For maintenance of CD8⁺ T cell depletion, injections were repeated every 2–3 d beginning on day 6. This regimen of administration resulted in approximately 95% depletion of CD8⁺ T cells from the peripheral blood and spleens of mice without tumors, as evaluated by flow cytometry (data not shown). This antibody was purified from ascites fluid produced in nude BALB/c mice (Cocalico Biologicals) inoculated with hybridoma cell line clone 53-6.72 (American Type Culture Collection) with a standard protocol of ammonium sulfate and caprylic acid precipitations. To ensure endotoxin-free antibody solution, a Detoxi-Gel Affinity Pack kit (Thermo Scientific, Pierce) was used for removal of lipopolysaccharide.

All compounds used for *in vivo* studies were tested to ensure they were lipopolysaccharide free.

Tissue processing, cell isolation and purification. Portions of tumors and spleens were fixed in 10% (vol/vol) formalin, were frozen in optimum cutting temperature medium at -70 °C or were used for cell isolation. Fixed samples were routinely processed for histological evaluation and immunohistochemical staining. Frozen samples were cut with a cryostat into sections 5 μ m in thickness for immunofluorescence staining. Blood samples, after erythrocyte lysis, were analyzed by flow cytometry for analysis of the expression of surface markers and C5aR by white blood cells. Portions of tumors and spleens were mechanically disaggregated to obtain single-cell suspensions. For removal of erythrocytes before cell culture or staining, cell suspensions were treated for 5 min on ice with 155 mM NH₄Cl, 10 mM KHCO₃ and 1 mM EDTA, pH 7.3. Myeloid precursors were selected by means of magnetic sorting as described¹⁰; single-cell suspensions from the tumors were preincubated with mAb to mouse CD16-CD32 (2.4G2; BD Biosciences) for blockade of Fc γ receptors. Cells were then incubated for 30 min with biotinylated anti-mouse Gr-1 (RB6-8C5; BD Biosciences), were washed and then were incubated for 30 min at 4 °C with BD IMag Streptavidin Particles Plus (BD Biosciences) and were separated with an IMagnet (BD Biosciences).

Complement deposition and immune cell infiltration. The deposition of C3 cleavage products in tumor tissue was detected with rat mAb to mouse C3 (2/11; HMI065; Hycult Biotechnology) as described⁵⁴. This mAb specifically recognizes epitopes of C3 cleavage products (C3b, iC3b and C3c) but not inactive C3. Therefore, positive reactivity in tissues is thought to be associated with activation of the complement cascade and C3 cleavage. The deposition of C1q and mannan-binding lectin was evaluated with rat mAb to mouse C1q (7H8; Abcam) and polyclonal goat antibody to mouse mannan-binding lectin (sc-17911; Santa Cruz Biotechnology), respectively. Sections were costained with biotinylated anti-mouse CD31 (MEC 13.3) for visualization of tumor vasculature. The infiltration of tumors with CD8⁺ T cells or myeloid-origin cells was analyzed with anti-mouse CD8 (53-6.7) or anti-mouse CD11b (MI/70), respectively. Isotype-matched rat IgG antibodies were used as a negative control. Anti-CD31, anti-CD8 and anti-CD11b and isotype-matched control antibodies

(559073 and 553987) were from BD Biosciences. Primary antibodies bound in tissue were detected with carbocyanine-conjugated donkey anti-rat or anti-goat (12-225-150, 712-165-150 and 705-225-003; The Jackson Laboratory), except anti-CD31, which was visualized with a streptavidin-rhodamine complex (BD Biosciences). Immunofluorescence staining was done on frozen sections 5 μ m in thickness. For detection of complement deposition, green and red fluorescence images were merged with the use of Spot software (Diagnostic Instruments). CD8⁺ tumor infiltrates were quantified with ImageJ image-analysis software (National Institutes of Health); CD8⁺ cells were counted in whole tissue sections and means were calculated. The magnitude of CD11b⁺ infiltrates was assessed in a semiquantitative way because of the relatively low numbers of infiltrating cells. Scores of 0–5 were assigned to sections according to the number of CD11b⁺ cells. In addition, the distribution of infiltrating cells was analyzed. All analyses were made by researchers 'blinded' to sample identity.

Flow cytometry. Single-cell suspensions were preincubated with mAb to mouse CD16-CD32 (Fc block; 2.4G2; BD Pharmingen) for blockade of Fc γ receptors, then they were incubated with primary antibody. Fluorochrome-conjugated mAbs to mouse CD3 (17A2), CD4 (L3T4), CD8 (53-6.7), CD11b (M1/70), CD25 (PC61), CD45 (30-F11), CD69 (H1.2F3) and Gr-1 (RB6-8C5; all from BD Biosciences) were used according to the manufacturer's instructions. For analysis of the cell surface expression of C5aR, cells were sequentially incubated with rabbit polyclonal anti-mouse C5aR (C1150-32; BD Biosciences) or rabbit isotype-matched control antibody (550875; BD Pharmingen) and fluorescein isothiocyanate-conjugated anti-rabbit IgG (F0112; R&D Systems) or with rat mAb to mouse C5aR (20/70; Hycult Biotechnology; Cell Science) or rat isotype-matched control antibody (553928; BD Pharmingen), followed by fluorescein isothiocyanate-conjugated anti-rat IgG (81-9511; Zymed-Invitrogen). In some experiments, cells were made permeable with Cytofix/Cytoperm and Perm/Wash buffers (BD Biosciences) before being stained for C5aR. Stained cells were analyzed by six-color flow cytometry on a FACSCanto (BD Biosciences) with FlowJo software (Tree Star).

Preparation of T cells labeled with the cytosolic dye CFSE. For proliferation studies, spleens were collected from naive C57BL/6J mice and were mechanically disrupted by passage through 100- μ m mesh cups to obtain single-cell suspensions. After lysis of red blood cells, the splenocytes were pooled, were pelleted by centrifugation and were washed twice in serum-free RPMI medium. Splenocytes were then labeled with CFSE (5-(and-6)-carboxyfluorescein succinimidyl ester; Molecular Probes) as follows: cells were washed with ice-cold PBS, were resuspended at a density of 5×10^6 cells per ml in ice-cold PBS and were labeled by dilution of the 0.5 mM CFSE stock 1,000-fold into the cell suspension (final concentration, 0.5 μ M) and incubation of the cells for 10 min at 37 °C. After labeling, FCS was added to a final concentration of 5% (vol/vol) and cells were immediately centrifuged and washed with ice-cold PBS.

Assay of the suppression of T cell proliferation. The suppressive effect of MDSCs on T cell proliferation was assessed in coculture assays as follows: CFSE-labeled splenocytes (1×10^5) were cultured together for 5 d at 37 °C with MDSCs (1×10^5) in the presence of phytohemagglutinin (5 μ g/ml; Sigma) in RPMI medium with 10% (vol/vol) FBS in an atmosphere of 5% CO₂. T cell proliferation was determined by flow cytometry. For this, nonadherent cells recovered from the cocultures were stained with fluorochrome-labeled anti-mouse CD3 (17A2; BD Bioscience) after blockade of Fc receptors. Dilution of the CFSE signal in the fluorescein isothiocyanate channel among CD3-gated cells was considered indicative of proliferation. CFSE-labeled splenocytes cultured with phytohemagglutinin in the absence of MDSCs (maximum proliferation; lowest CFSE signal) and unstimulated splenocytes labeled in the same way (basal proliferation; highest CFSE signal) were used as controls.

Production of ROS and RNS The oxidation-sensitive dye H₂DCFDA (2'-7'-dichloro dihydrofluorescein diacetate; Molecular Probes) was used for measurement of the production of ROS and RNS in cells isolated from tumors or spleens. Excised tumors and spleens were mechanically disintegrated to obtain a single-cell suspension. Cells resuspended in DMEM were incubated for 15 min at 37 °C with 2 μ M dye. After being washed with PBS, cells were stained for flow cytometry as described above. MDSCs were distinguished from other cells in the suspension as a viable CD45⁺CD11b⁺Gr-1⁺ population, and fluorescence

intensity was estimated in the channel suitable for fluorescein isothiocyanate according to the manufacturer's instruction (Molecular Probes). The amount of ROS and RNS in cells was proportional to the intensity of fluorescence and is expressed as median fluorescence for gated populations. For some experiments, in addition to being incubated with H₂DCFDA, freshly isolated cells were simultaneously stimulated with 1, 10 or 100 nM recombinant mouse C5a expressed as described⁵⁵ or with 1 μ M PMA (Sigma-Aldrich). Preliminary experiments have shown that stimulation of cells with 10 nM C5a produces the highest induction of ROS and RNS production.

Statistics. The effect of genotype or treatment on tumor growth (Figs. 1–4 and Supplementary Fig. 1) was evaluated by two-way analysis of variance (ANOVA) with GraphPad Prism (GraphPad Software); the Bonferroni post-test correction was applied to control for the occurrence of false-positive results. For evaluation of the significance of the correlation between tumor volumes and cell infiltrates (Figs. 4,5 and Supplementary Fig. 3) or arginase concentration (Fig. 7), the Pearson correlation test was applied (GraphPad Prism). An unpaired two-tailed Student's *t*-test (Microsoft Excel) was used for testing the significance of differences in the percentages of MDSCs in tumors and spleens (Fig. 5i–k), for assays of tumor cell proliferation and apoptosis and micro-vascular density (Supplementary Fig. 2) and for analysis of the number of T cells in CD8⁺ T cell-depleted mice (Supplementary Fig. 3). To determine whether induction of CD11b (Fig. 6) or ROS (Fig. 7) over baseline values (set as 1) was significant, the one-sample *t*-test was used (GraphPad Prism). The Wilcoxon signed-rank test (GraphPad Prism) was applied for evaluation of the significance of differences in median fluorescence values proportional to the production of ROS and RNS by MDSCs (Fig. 7). *P* values of 0.05 or less were considered significant.

Additional methods. Information on cell proliferation, apoptosis and angiogenesis, quantitative real-time PCR analysis, the preparation of dendritic cells and macrophages, and immunoblot analysis is available in the Supplementary Methods online.

Accession code. UCSD-Nature Signaling Gateway (<http://www.signaling-gateway.org>): A000037.

Note: Supplementary information is available on the Nature Immunology website.

ACKNOWLEDGMENTS

We thank R.A. Wetsel (University of Texas, Houston) for C3 and factor B-deficient mice; D. Ricklin and C. Tsoukas for critical review of the manuscript; D. McClellan for editorial assistance; the Morphology Core of the Penn Center for Molecular Studies in Digestive and Liver Diseases for technical assistance; Hycult Biotechnology for mAb to C3; and P. Magotti (University of Pennsylvania, Philadelphia) for mouse C5a and for characterizing the C5aR antagonist and control peptide. Supported by the US National Institutes of Health (CA112162-03, GM62134 and A1068730 to J.D.L.).

AUTHOR CONTRIBUTIONS

M.M.M. designed and did experiments, analyzed data and wrote the manuscript; R.A.D. contributed to *in vivo* experiments, data analysis and writing the manuscript; F.B. did T cell proliferation assays and PCR analysis and contributed to flow cytometry experiments; S.K.R.-L. and A.K. contributed to *in vivo* and flow cytometry experiments; C.G. provided C5aR-deficient mice and advice for the project; G.C. provided advice for the project and reviewed the manuscript; and J.D.L. conceived and supervised the project and coordinated the writing of the manuscript.

COMPETING INTERESTS STATEMENT

The authors declare competing financial interests: details accompany the full-text HTML version of the paper at <http://www.nature.com/natureimmunology/>.

Published online at <http://www.nature.com/natureimmunology/>
Reprints and permissions information is available online at <http://npg.nature.com/reprintsandpermissions/>

- Dunn, G.P., Bruce, A.T., Ikeda, H., Old, L.J. & Schreiber, R.D. Cancer immunoeediting: from immunosurveillance to tumor escape. *Nat. Immunol.* **3**, 991–998 (2002).
- Swann, J.B. & Smyth, M.J. Immune surveillance of tumors. *J. Clin. Invest.* **117**, 1137–1146 (2007).

3. Coussens, L.M. & Werb, Z. Inflammation and cancer. *Nature* **420**, 860–867 (2002).
4. Balkwill, F. & Mantovani, A. Inflammation and cancer: back to Virchow? *Lancet* **357**, 539–545 (2001).
5. Bhardwaj, N. Harnessing the immune system to treat cancer. *J. Clin. Invest.* **117**, 1130–1136 (2007).
6. Lin, W.W. & Karin, M. A cytokine-mediated link between innate immunity, inflammation, and cancer. *J. Clin. Invest.* **117**, 1175–1183 (2007).
7. Blank, C. *et al.* PD-L1/B7H-1 inhibits the effector phase of tumor rejection by T cell receptor (TCR) transgenic CD8⁺ T cells. *Cancer Res.* **64**, 1140–1145 (2004).
8. Dong, H. *et al.* Tumor-associated B7–H1 promotes T-cell apoptosis: a potential mechanism of immune evasion. *Nat. Med.* **8**, 793–800 (2002).
9. Sica, A. & Bronte, V. Altered macrophage differentiation and immune dysfunction in tumor development. *J. Clin. Invest.* **117**, 1155–1166 (2007).
10. Kusmartsev, S., Nagaraj, S. & Gabrilovich, D.I. Tumor-associated CD8⁺ T cell tolerance induced by bone marrow-derived immature myeloid cells. *J. Immunol.* **175**, 4583–4592 (2005).
11. Kusmartsev, S., Nefedova, Y., Yoder, D. & Gabrilovich, D.I. Antigen-specific inhibition of CD8⁺ T cell response by immature myeloid cells in cancer is mediated by reactive oxygen species. *J. Immunol.* **172**, 989–999 (2004).
12. Marx, J. Cancer immunology. Cancer's bulwark against immune attack: MDS cells. *Science* **319**, 154–156 (2008).
13. Markiewski, M.M. & Lambris, J.D. The role of complement in inflammatory diseases from behind the scenes into the spotlight. *Am. J. Pathol.* **171**, 715–727 (2007).
14. Carroll, M.C. The complement system in regulation of adaptive immunity. *Nat. Immunol.* **5**, 981–986 (2004).
15. Sahu, A. *et al.* Structure, functions, and evolution of the third complement component and viral molecular mimicry. *Immunol. Res.* **17**, 109–121 (1998).
16. Guo, R.F. & Ward, P.A. Role of C5a in inflammatory responses. *Annu. Rev. Immunol.* **23**, 821–852 (2005).
17. Gorter, A. & Meri, S. Immune evasion of tumor cells using membrane-bound complement regulatory proteins. *Immunol. Today* **20**, 576–582 (1999).
18. Niculescu, F., Rus, H.G., Retegan, M. & Vlaicu, R. Persistent complement activation on tumor cells in breast cancer. *Am. J. Pathol.* **140**, 1039–1043 (1992).
19. Donin, N. *et al.* Complement resistance of human carcinoma cells depends on membrane regulatory proteins, protein kinases and sialic acid. *Clin. Exp. Immunol.* **131**, 254–263 (2003).
20. Macor, P. & Tedesco, F. Complement as effector system in cancer immunotherapy. *Immunol. Lett.* **111**, 6–13 (2007).
21. Gelderman, K.A., Tomlinson, S., Ross, G.D. & Gorter, A. Complement function in mAb-mediated cancer immunotherapy. *Trends Immunol.* **25**, 158–164 (2004).
22. Lin, K.Y. *et al.* Treatment of established tumors with a novel vaccine that enhances major histocompatibility class II presentation of tumor antigen. *Cancer Res.* **56**, 21–26 (1996).
23. Sahu, A. & Lambris, J.D. Structure and biology of complement protein C3, a connecting link between innate and acquired immunity. *Immunol. Rev.* **180**, 35–48 (2001).
24. Monk, P.N., Scola, A.M., Madala, P. & Fairlie, D.P. Function, structure and therapeutic potential of complement C5a receptors. *Br. J. Pharmacol.* **152**, 429–448 (2007).
25. Finch, A.M. *et al.* Low-molecular-weight peptidic and cyclic antagonists of the receptor for the complement factor C5a. *J. Med. Chem.* **42**, 1965–1974 (1999).
26. Holtz, D.O. *et al.* Should tumor VEGF expression influence decisions on combining low-dose chemotherapy with antiangiogenic therapy? Preclinical modeling in ovarian cancer. *J. Transl. Med.* **6**, 2 (2008).
27. Johswich, K. *et al.* Ligand specificity of the anaphylatoxin C5L2 receptor and its regulation on myeloid and epithelial cell lines. *J. Biol. Chem.* **281**, 39088–39095 (2006).
28. Movahedi, K. *et al.* Identification of discrete tumor-induced myeloid-derived suppressor cell subpopulations with distinct T-cell suppressive activity. *Blood* **111**, 4233–4244 (2008).
29. Mollnes, T.E. *et al.* Essential role of the C5a receptor in *E. coli*-induced oxidative burst and phagocytosis revealed by a novel leprudin-based human whole blood model of inflammation. *Blood* **100**, 1869–1877 (2002).
30. Daniel, D.S. *et al.* The reduced bactericidal function of complement C5-deficient murine macrophages is associated with defects in the synthesis and delivery of reactive oxygen radicals to mycobacterial phagosomes. *J. Immunol.* **177**, 4688–4698 (2006).
31. Guo, R.F. *et al.* Neutrophil C5a receptor and the outcome in a rat model of sepsis. *FASEB J.* **17**, 1889–1891 (2003).
32. de Visser, K.E., Korets, L.V. & Coussens, L.M. Early neoplastic progression is complement independent. *Neoplasia* **6**, 768–776 (2004).
33. Huber-Lang, M. *et al.* Generation of C5a in the absence of C3: a new complement activation pathway. *Nat. Med.* **12**, 682–687 (2006).
34. Shankaran, V. *et al.* IFN- γ and lymphocytes prevent primary tumour development and shape tumour immunogenicity. *Nature* **410**, 1107–1111 (2001).
35. Smyth, M.J. *et al.* Perforin-mediated cytotoxicity is critical for surveillance of spontaneous lymphoma. *J. Exp. Med.* **192**, 755–760 (2000).
36. Hawlisch, H. & Kohl, J. Complement and Toll-like receptors: key regulators of adaptive immune responses. *Mol. Immunol.* **43**, 13–21 (2006).
37. Suresh, M. *et al.* Complement component 3 is required for optimal expansion of CD8⁺ T cells during a systemic viral infection. *J. Immunol.* **170**, 788–794 (2003).
38. Kim, A.H. *et al.* Complement C5a receptor is essential for the optimal generation of antiviral CD8⁺ T cell responses. *J. Immunol.* **173**, 2524–2529 (2004).
39. Liu, J. *et al.* The complement inhibitory protein DAF (CD55) suppresses T cell immunity in vivo. *J. Exp. Med.* **201**, 567–577 (2005).
40. Kohl, J. & Wills-Karp, M. Complement regulates inhalation tolerance at the dendritic cell/T cell interface. *Mol. Immunol.* **44**, 44–56 (2007).
41. Kohl, J. *et al.* A regulatory role for the C5a anaphylatoxin in type 2 immunity in asthma. *J. Clin. Invest.* **116**, 783–796 (2006).
42. Karp, C.L. *et al.* Identification of complement factor 5 as a susceptibility locus for experimental allergic asthma. *Nat. Immunol.* **1**, 221–226 (2000).
43. Peng, T. *et al.* Role of C5 in the development of airway inflammation, airway hyperresponsiveness, and ongoing airway response. *J. Clin. Invest.* **115**, 1590–1600 (2005).
44. Gallina, G. *et al.* Tumors induce a subset of inflammatory monocytes with immunosuppressive activity on CD8⁺ T cells. *J. Clin. Invest.* **116**, 2777–2790 (2006).
45. Mastellos, D. & Lambris, J.D. Complement: more than a 'guard' against invading pathogens? *Trends Immunol.* **23**, 485–491 (2002).
46. Mantovani, A., Romero, P., Palucka, A.K. & Marincola, F.M. Tumour immunity: effector response to tumour and role of the microenvironment. *Lancet* **371**, 771–783 (2008).
47. Kohl, J. Drug evaluation: the C5a receptor antagonist PMX-53. *Curr. Opin. Mol. Ther.* **8**, 529–538 (2006).
48. Ricklin, D. & Lambris, J.D. Complement-targeted therapeutics. *Nat. Biotechnol.* **25**, 1265–1275 (2007).
49. Circolo, A. *et al.* Genetic disruption of the murine complement C3 promoter region generates deficient mice with extrahepatic expression of C3 mRNA. *Immunopharmacology* **42**, 135–149 (1999).
50. Wessels, M.R. *et al.* Studies of group B streptococcal infection in mice deficient in complement component C3 or C4 demonstrate an essential role for complement in both innate and acquired immunity. *Proc. Natl. Acad. Sci. USA* **92**, 11490–11494 (1995).
51. Matsumoto, M. *et al.* Abrogation of the alternative complement pathway by targeted deletion of murine factor B. *Proc. Natl. Acad. Sci. USA* **94**, 8720–8725 (1997).
52. Hopken, U.E., Lu, B., Gerard, N.P. & Gerard, C. The C5a chemoattractant receptor mediates mucosal defence to infection. *Nature* **383**, 86–89 (1996).
53. Holland, M.C., Morikis, D. & Lambris, J.D. Synthetic small-molecule complement inhibitors. *Curr. Opin. Investig. Drugs* **5**, 1164–1173 (2004).
54. Mastellos, D. *et al.* Novel monoclonal antibodies against mouse C3: Description of fine specificity and applications to various immunoassays. *Mol. Immunol.* **40**, 1213–1221 (2004).
55. Strey, C.W. *et al.* The proinflammatory mediators C3a and C5a are essential for liver regeneration. *J. Exp. Med.* **198**, 913–923 (2003).